



# Controllable synthesis of patchy particles with tunable geometry and orthogonal chemistry

Fuqiang Chang<sup>a</sup>, Samia Ouhajji<sup>a,1</sup>, Alice Townsend<sup>a</sup>, Kanvaly Sanogo Lacina<sup>a</sup>, Bas G.P. van Ravensteijn<sup>b,c</sup>, Willem K. Kegel<sup>a,\*</sup>

<sup>a</sup> Van't Hoff Laboratory for Physical and Colloid Chemistry, Debye Institute for Nanomaterials Science, Utrecht University, 3584 CH Utrecht, The Netherlands

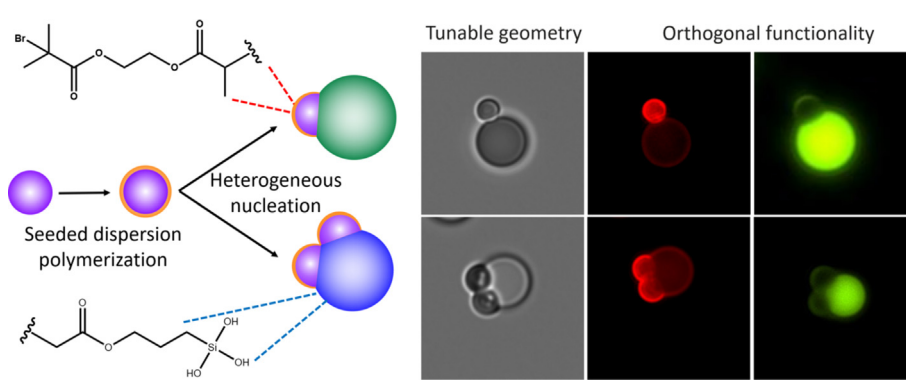
<sup>b</sup> Institute for Complex Molecular Systems, Eindhoven University of Technology, P.O. Box 513, 5600 MB, Eindhoven, The Netherlands

<sup>c</sup> Department of Chemical Engineering and Chemistry, Eindhoven University of Technology, P.O. Box 513, 5600 MB, Eindhoven, The Netherlands

## HIGHLIGHTS

- Anisotropic colloids carrying chemically orthogonal patches were synthesized.
- Both types of patches could be functionalized independently and site-specifically.
- Controlling patch chemistry and geometry opens new avenues for colloidal assembly.

## GRAPHICAL ABSTRACT



## ARTICLE INFO

### Article history:

Received 6 July 2020

Revised 9 August 2020

Accepted 10 August 2020

Available online 12 August 2020

### Keywords:

Anisotropic colloids

Patchy particles

Colloidal molecules

Heterogeneous nucleation

Orthogonal chemistry

## ABSTRACT

**Hypothesis:** Self-assembly using anisotropic colloidal building blocks may lead to superstructures similar to those found in molecular systems yet can have unique optical, electronic, and structural properties. To widen the spectrum of achievable superstructures and related properties, significant effort was devoted to the synthesis of new types of colloidal particles. Despite these efforts, the preparation of anisotropic colloids carrying chemically orthogonal anchor groups on distinct surface patches remains an elusive challenge.

**Experiments:** We report a simple yet effective method for synthesizing patchy particles via seed-mediated heterogeneous nucleation. Key to this procedure is the use of 3-(trimethoxysilyl)propyl methacrylate (TPM) or 3-(trimethoxysilyl)propyl acrylate (TMSPA), which can form patches on a variety of functional polymer seeds via a nucleation and growth mechanism.

**Findings:** A family of anisotropic colloids with tunable numbers of patches and patch arrangements were prepared. By continuously feeding TPM or TMSPA the geometry of the colloids could be adjusted accurately. Furthermore, the patches could be reshaped by selectively polymerizing and/or solvating the individual colloidal compartments. Relying on the chemically distinct properties of the TPM/TMSPA and seed-derived domains, both types of patches could be functionalized independently. Combining detailed control over the patch chemistry and geometry opens new avenues for colloidal self-assembly.

© 2020 The Author(s). Published by Elsevier Inc. This is an open access article under the CC BY license (<http://creativecommons.org/licenses/by/4.0/>).

\* Corresponding author.

E-mail address: [w.k.kegel@uu.nl](mailto:w.k.kegel@uu.nl) (W.K. Kegel).

<sup>1</sup> Current address: Soft Matter Physics, Huygens-Kamerlingh Onnes Laboratory, Leiden University, PO Box 9504, 2300 RA Leiden, The Netherlands.

## 1. Introduction

Analogous to atoms and molecules, colloidal particles under thermal agitation are able to spontaneously assemble into larger superstructures. Therefore, (anisotropic) colloids have been regarded as important model systems to study the molecular and/or atomistic world. Moreover, because of their size and surface properties, new types of materials can in principle be created by using colloids as building blocks. Crucial for the successful bottom-up construction of complex assemblies is access to elementary building blocks with well-designed shapes that interact with each other in a highly directional manner. To embed these characteristics in colloidal particles, intensive research has been devoted to tailor the size, shape and surface characteristics of colloidal particles [1,2]. Dispersion and emulsion polymerization-based techniques have been widely used to prepare anisotropic particles in a scalable manner [3–6]. Typically, cross-linked spherical seed particles are swollen with monomer(s). Subsequently, the swelling monomer undergoes a (heat-induced) phase separation from the cross-linked polymer network to form an additional lobe on the surface of the seed particles. This phase separation is driven by an elastic stress that is generated upon contraction of the cross-linked polymer network. While large quantities of anisotropic colloids can be produced by this method, a severe drawback of these procedures is the restriction in attainable particle morphologies. The underlying reason for this limited geometric variation is directly coupled to the phase separating mechanism by which the patches are formed. To generate sufficient elastic stress to drive the phase separation, a minimum amount of swelling monomer needs to be used. The introduction of patches small compared to the size of the seeds is therefore challenging. On the other end of the geometric spectrum, the protrusion size is limited by the maximum swelling capacity of the seed particles [7,8]. In addition to the limitations in particle anisotropy, seeded polymerizations can only be employed with monomers that are compatible with the cross-linked seed, *i.e.*, that are able to swell the polymer matrix. This severely limits the chemical freedom in generating particles with distinct lobes.

Alternatively, seed-mediated heterogeneous nucleation and growth methods have been proposed as an efficient strategy for synthesizing anisotropic particles. Sacanna *et al.* [9–11] prepared a whole “zoo” of anisotropic colloids using colloidal seeds to induce the heterogeneous nucleation of hydrolyzed 3-methacryloxypropyl trimethoxysilane (TPM) monomers. During synthesis, the TPM condenses on the seed particles, forming a liquid droplet. This droplet can be easily solidified by polymerization to yield the desired anisotropic colloids. The size of the nucleated TPM droplets is in principle not limited by synthetic constraints. Indeed, it was found that by controlling the TPM concentration a wide variation in patch sizes could be obtained [12].

Although these *state-of-the-art* synthetic procedures provide good control over the particle morphology, the resulting colloids generally feature at least one patch that is “inert” towards conventional chemical modification procedures, [3,6,13] or patches that contain identical functionality [14–17]. A synthetic hurdle that has yet to be taken to truly expand the attainable structural diversity upon assembly is the synthesis of anisotropic particles that carry patches which can be modified in a truly orthogonal manner.

Inspired by the work of Sacanna *et al.*, we introduce a general route towards bifunctional anisotropic colloids with chemically orthogonal functional patches by combining seeded dispersion polymerizations with patch formation *via* heterogeneous nucleation. Functional core–shell seeds synthesized using seeded dispersion polymerization were converted into single-patch (dumbbell-like) or double-patch (trimer-shape) colloids by

heterogeneous nucleation of silane alkoxide monomers (TPM or 3-(trimethoxysilyl)propyl acrylate (TMSPA)) on their surface. The size ratio, morphology, and geometry of the anisotropic particles could be controlled by the TPM/TMSPA feeding ratio. As the chemical characteristics of the seed particles are distinctly different from the TPM or TMSPA-derived lobes, both types of patches could be independently modified. The combined geometric and site-specific chemical control reported here is a significant step forwards to the next-generation of colloidal model systems for (self-)assembly.

## 2. Experimental section

**Materials.** Styrene (St, 99%), 2-(2-bromoisobutyryloxy)ethyl methacrylate (BIEM, 95%), 2-hydroxyethyl acrylate (HEA, 96%, contains 200–650 ppm monomethyl ether hydroquinone as inhibitor), sodium 4-styrenesulfonate (NaSS), toluene (techn., Interchem), (3-aminopropyl)triethoxysilane (APS, 99%), Ficoll (PM 400), fluorescein isothiocyanate (FITC, 90%), hexamethyldisilazane (HMDS, 99%), methacryloxyethyl thiocarbonyl rhodamine B (MTR), copper bromide (Cu(I)Br, 98%), bromotris(triphenylphosphine)copper (I) (CuBr(PPh<sub>3</sub>)<sub>3</sub>, 98%) and *N,N,N',N',N'*-pentamethyldiethylenetriamine (PMDETA, 99%) were obtained from Sigma Aldrich. Sodium bisulfite (NaHSO<sub>3</sub>, ACS reagent), 3-(trimethoxysilyl)propyl methacrylate (TPM, 98%), 3-(trimethoxysilyl)propyl acrylate (TMSPA, 92%) and  $\alpha,\alpha'$ -azobis(isobutyronitrile) (AIBN, 98%) were purchased from Acros Organics. 1-Butanol (BuOH, 99%) and sodium azide (NaN<sub>3</sub>, 99%) were purchased from Fisher Scientific. Ammonium hydroxide (for analysis, 28–30 wt%) was purchased from Antonides CV. Ethanol (EtOH, p.a., ACS reagent) was purchased from Merck. Methanol (MeOH, ACS specifications) was obtained from J. T. Baker. The water used for all syntheses was purified using a Milli-Q system. All chemicals were used without further purification.

**Synthesis of linear charge-stabilized polystyrene (PS).** Linear micron-sized polystyrene spheres were synthesized using a stabilizer-free dispersion polymerization method as described in the literature [18]. St (8 mL, 70 mmol), NaSS (0.13 g, 0.63 mmol), and AIBN (90 mg, 0.55 mmol) were dissolved in a mixture of water (10 mL) and EtOH (40 mL) in a 100 mL round-bottom flask. The flask was sealed with a stopper and then flushed with N<sub>2</sub> for 30 min. Polymerization was carried out by immersing the flask in an oil bath of 70 °C for 20 h under magnetic stirring. The resulting dispersion was washed by centrifugation and redispersion in water (3 × ) to remove remaining monomers/oligomers. Particles with an average diameter of 1.2 μm and polydispersity of 2% were obtained according to transmission electron microscopy (TEM) (Fig. S2).

**Synthesis of functional polystyrene particles (PS-Br).** A dispersion containing PS colloids (20 mL, solid content = 18 wt%) was charged into a 250 mL round-bottom flask, followed by the addition of water (100 mL) yielding a 3 wt% dispersion. The reaction flask was subjected to ultra-sonication for 20 min to ensure all colloids were fully dispersed. A solution comprising St (2.5 mL, 22 mmol), BIEM (1.1 mL, 5 mmol), and AIBN (35 mg, 0.2 mmol) was added. The sample was then rotated under a 60° angle for 12 h in order to facilitate the swelling of the colloids with the added monomers. After this swelling period, polymerization was carried out by immersing the flask in an oil bath of 75 °C at an angle of 60° and rotating it at ~100 rpm. After 12 h of polymerization, the dispersion was washed by centrifugation and redispersion with water (3 × ). The resulting particles had a diameter of 1.5 μm and a polydispersity of 5% as determined with transmission electron microscopy (TEM). Incorporation of BIEM was confirmed with infrared (IR) spectroscopy (Fig. S1).

**Synthesis of hybrid patchy particles from functional spheres (PS-Br-TPM/PS-Br-TMSPA).** In a typical experiment, TPM (1 mL, 4 mmol), was hydrolyzed in water (10 mL) by vigorous stirring for approximately 5 h. For TMSPA hydrolysis, 0.5 mL was added to water (15 mL) and stirred for 5 h. Next, hydrolyzed TPM/TMSPA solution (3 mL, h-TPM or h-TMSPA) and ammonium hydroxide (1  $\mu$ L, 28 wt%) were rapidly mixed with a dispersion containing the brominated seed spheres (15 mL, 0.5 wt%) in a 40 mL glass vial. The mixture was left undisturbed for up to 2 h to allow the TPM to nucleate on the surface of the seed particles. Colloids with the desired size ratio were obtained by feeding h-TPM or h-TMSPA to the crude reaction system. Finally, to solidify the TPM/TMSPA lobe, AIBN (210 mg, 1.3 mmol) was added to polymerize the droplet at 80 °C for 16 h.

**Reshaping the PS phase of the anisotropic particles.** After nucleation of the TPM/TMSPA droplets, the spherical PS seeds were plasticized and progressively deformed by adding small amounts of toluene (typically on the order of 125  $\mu$ L of toluene per 30 mL as-prepared crude dispersion). The dispersions were then left under mild stirring for 3 h and the changes in morphology were followed by optical microscopy.

To selectively dissolve the linear polystyrene core, a solvent mixture of toluene (125  $\mu$ L) and EtOH (625  $\mu$ L) per 30 mL dispersion was used. After chemical etching, the colloidal structures were fixed by stirring the suspension at 80 °C in an open container and allowing the toluene and EtOH to evaporate.

To prepare particles with a smooth p(TPM)/p(TMSPA) patch and rough PS-Br lobes, the patchy particles were exposed to a second heterogeneous nucleation. Typically, h-TPM or h-TMSPA solution (1 mL) and ammonium hydroxide (5  $\mu$ L, 28 wt%) were rapidly mixed with a dispersion containing the patchy particles (18 mL, solid content = 0.5 wt%) in a 40 mL glass vial before solidification. The sample was then left for several hours to obtain particles with the desired roughness. The TPM/TMSPA patches were solidified *via* free radical polymerization by addition of AIBN (70 mg, 0.4 mmol) and heating at 80 °C for 16 h.

**Post-modification of seed-derived lobes.** Atom transfer radical polymerization (ATRP) was used to graft HEA from the brominated patches following a procedure which was adapted from reference [19]. HEA (180  $\mu$ L, 1.6 mmol) and Cu(I)Br (25 mg, 0.17 mmol) were added directly into an oven dried Schlenk flask. For labelling experiments, the monomer mixture consisted of HEA mixed with MTR (2 mg, 0.003 mmol). An EtOH/H<sub>2</sub>O mixture (1:1, v/v) (1 mL) was added to the reaction flask and the solution was stirred for 10 min to dissolve the Cu(I)Br, resulting in the appearance of a light grey-green color. Subsequently, PMDETA (120  $\mu$ L, 0.6 mmol) was injected into the reaction mixture. Upon addition of PMDETA, the reaction mixture turned light green. The mixture was degassed by evacuation and refilling with N<sub>2</sub> repeatedly (3  $\times$ ). In a separate Schlenk flask, the PS-Br-TPM or PS-Br-TMSPA particles dispersed in the EtOH/H<sub>2</sub>O mixture (1:1, v/v) (1 mL, solid content = 1 wt%) were degassed. The degassed particle dispersion was injected into the monomer/catalyst mixture under N<sub>2</sub> atmosphere. The light green reaction mixture was allowed to stir for 10 h at 40 °C (labelling experiments were performed in the dark and quenched after 20 min). The resulting particles were washed several times with EtOH, 50 mM NaSO<sub>3</sub> solution (to promote removal of the copper catalyst) and water, respectively.

To substitute the bromides on PS-Br-TPM for azides the following procedure was performed. PS-Br-TPM dispersed in BuOH/H<sub>2</sub>O mixture (7:3 v/v) (3 mL, solid content = 1 wt%), NaN<sub>3</sub> (23 mg, 0.35 mmol), and CuBr(PPh<sub>3</sub>)<sub>3</sub> (8.9 mg, 0.01 mmol) were added in a glass vial. The reaction mixture was stirred at 70 °C for 14 h. Subsequently, the azide functionalized anisotropic particles were washed with ethanol and water (3  $\times$ ).

**Post-modification of poly(TPM) lobes.** To confirm the functionality of the TPM/TMSPA lobes, a rhodamine-based fluorescent silane coupling agent was used to covalently label the surface of these patches [20]. This fluorescent coupling agent was obtained by dissolving RITC (7.5 mg, 0.014 mmol) and APS (0.8 mL, 3.61 mmol) in EtOH (10 mL). The resulting stock solution was stirred overnight in the dark at room temperature and then stored at 4 °C. The dye solution (20  $\mu$ L) was added into a 4 mL glass vial containing the anisotropic particles dispersion in ethanol (1 mL, solid content = 0.5 wt%). The mixture was allowed to react in the dark for 24 h. The labeled particles were washed with EtOH and water (3  $\times$ ).

To modify the silane patches to be hydrophobic and to render the particle's functional groups detectable with IR spectroscopy after surface modification, HMDS was selected as the silane coupling agent [21]. Anisotropic particles (4 mg) dispersed in water were centrifuged and redispersed in ethanol (5  $\times$ ) and then dispersed in ethanol (1 mL) containing HMDS (8  $\mu$ L, 0.04 mmol). The samples were left on a roller table for at least 48 h at room temperature. After modification, the resulting particles were washed several times with EtOH to remove unreacted HMDS.

**Purification of anisotropic particles.** To separate the target particles from secondary p(TPM)/p(TMSPA) nuclei and non-reacted seeded spheres, the crude dispersions were purified using density gradient centrifugation [22]. A 30 mL continuous gradient of 8–20 wt% Ficoll was prepared in a centrifuge tube. Crude sample dispersion (1 mL, solid content = 0.5 wt%) was added on top of the Ficoll gradient solution. The sample was then centrifuged at 150  $\times$  g for 15 min until multiple bands appeared. Each band was removed separately using a syringe and washed with water at 1450  $\times$  g for 45 s (5  $\times$ ).

**Characterization.** Transmission electron microscope (TEM) images were taken with a Philips Tecnai10 electron microscope typically operating at 100 kV. The samples were prepared by drying a drop of diluted aqueous dispersion on top of polymer-coated copper grids. Scanning electron microscopy (SEM) samples were prepared using the same method. However, to achieve SEM images with higher magnification, a sputter coater with a platinum target was used to coat the dried copper grids. The samples were sputter-coated with a 10 nm thick platinum layer. SEM images were taken with a Philips SEM XL PEG 30 typically operating at 5–10 kV. Optical microscopy and fluorescence images ( $\lambda_{\text{excitation}} = 480$  nm for FITC and  $\lambda_{\text{excitation}} = 540$  nm for RITC) were taken with a Nikon Ti-E inverted microscope. Samples were prepared by placing a drop of the diluted dispersion on a microscopy slide. Infrared (IR) spectra were obtained using a PerkinElmer Frontier FT-IR/FIR spectrometer in attenuated total reflectance (ATR) mode. Measurements were taken on powders obtained by drying the sample dispersion.

### 3. Results and discussion

**Synthesis of single-patch particles with tunable size ratio.** A schematic overview of the synthetic strategy towards the bifunctional PS-Br-TPM particles is shown in Fig. 1. The method comprises three main steps. Firstly, functional core-shell spheres are synthesized *via* seeded dispersion polymerization. These particles are subsequently used as seeds to induce the heterogeneous nucleation of TPM or TMSPA. Finally, the surface-nucleated droplets are polymerized to yield the targeted anisotropic particles. The as prepared colloids consist of a highly cross-linked TPM/TMSPA patch [9], and a linear (non-cross-linked) polymeric core-shell seed. The synthetic procedure will be outlined in more detail below.

First, uniform charge-stabilized linear polystyrene (PS) microspheres were synthesized using stabilizer-free dispersion



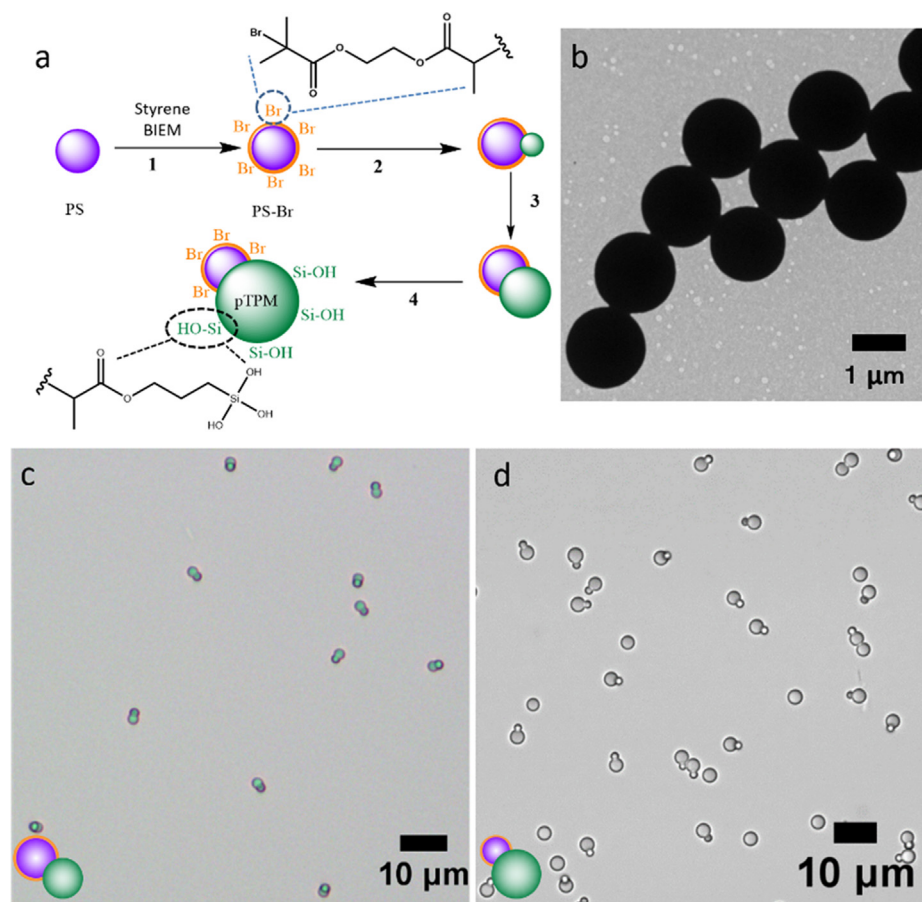


**Fig. 1.** (a) Schematic representation of the synthesis of anisotropic particles with two functional patches. Step (1): introduction of a functional shell (in orange) *via* seeded dispersion polymerization. The linear polystyrene seeds (purple) were swollen with a monomer mixture of 2-(2-bromoisobutyryloxy) ethyl methacrylate (BIEM) and styrene, and subsequently polymerized yielding brominated core-shell particles (PS-Br). Step (2): spherical seeds are partially engulfed in poly(3-(trimethoxysilyl)propyl methacrylate) p(TPM) oil droplets (in green) *via* seeded heterogeneous nucleation. Step (3): the TPM oil droplet grows into the desired size by feeding fresh hydrolyzed TPM (h-TPM). Step (4): a radical polymerization solidifies the TPM lobe, resulting in snowman-shaped colloids. (b) Transmission electron microscope (TEM) images of PS-Br core-shell seed particles. Representative optical microscope images of density-gradient centrifugation purified (c) symmetric and (d) asymmetric single-patch particles. In the latter case, the p(TPM) lobes are larger than the polystyrene-based patches.

polymerization using sodium 4-styrenesulfonate (NaSS) as charged comonomer. NaSS will preferentially partition at the surface of the colloidal particles, giving the particles a negative surface charge. In contrast to conventional dispersion polymerizations, which rely on steric stabilization *via* surface-adsorption of polymers, the use of NaSS ensures colloidal stability *via* the incorporation of permanently charged sulfonate moieties. The absence of polymeric stabilizers promotes the accessibility of the colloidal surface and therefore facilitates surface modifications [23]. The obtained particles with a diameter of 1.2  $\mu\text{m}$  and a polydispersity of 2% were subsequently swollen with styrene (St) and 2-(2-bromoisobutyryloxy) ethyl methacrylate (BIEM). BIEM was selected as functional comonomer to be able to modify the seed-derived patches using controlled polymer grafting after TPM nucleation as will be described later. It is noteworthy that seeded polymerization is a widely employed strategy to functionalize colloids and the procedure is not limited to BIEM only. Core-shell particles using (slightly) hydrophilic comonomers such as 2-(2-bromoisobutyryloxy) ethyl methacrylate, [24] 4-vinylbenzyl chloride, [13] and vinyl acetate [25,26] were reported before. These particles could in principle also be employed as seeds to produce similar patchy particles outlined here (see Supporting information S1).

After polymerization of the swelling monomers, a brominated copolymer shell was formed around the PS core (PS-Br). After seeded growth, uniform spherical particles with a diameter of

1.5  $\mu\text{m}$  and a polydispersity of 5% were obtained (Fig. 1b). Incorporation of BIEM was confirmed by infrared (IR) spectroscopy (Fig. S1). Comparison of the IR spectra of the bare PS and PS-Br particles revealed the appearance of a new band at  $1730\text{ cm}^{-1}$ . This band is diagnostic for the carbonyl vibration ( $\text{C}=\text{O}$ ) from the incorporated BIEM (Fig. 5).

Next, PS-Br served as seeds for the synthesis of the targeted patchy particles (Fig. 1, Step 2) by heterogeneous nucleation of TPM. Prior to addition, the TPM was hydrolyzed. This procedure yields metastable water-soluble silanols after a slow hydrolysis of the alkoxy silanes. Adding pre-hydrolyzed TPM (h-TPM) to PS-Br in alkaline conditions, induces rapid condensation reactions of the h-TPM. The formed oligomers are insoluble and preferably condense onto the seed particles generating liquid TPM protrusions [27]. Finally, the newly formed lobes were solidified by a heat-induced polymerization of the TPM oligomers through their methacrylate moieties, achieving single-patch organo-silica hybrid particles. The patchy colloids (Fig. 1c, d) were isolated from the crude reaction mixture which also contained a small fraction of spherical polystyrene seeds and p(TPM) secondary nuclei (Fig. S3).

By taking advantage of the nucleation-and-growth mechanism for protrusion formation and the fact that the TPM lobes remain liquid before polymerization, we explored the possibilities to tune the dimensions of the TPM domain. As shown in Fig. 2, for a given size of functional seed particles, we were able to control the

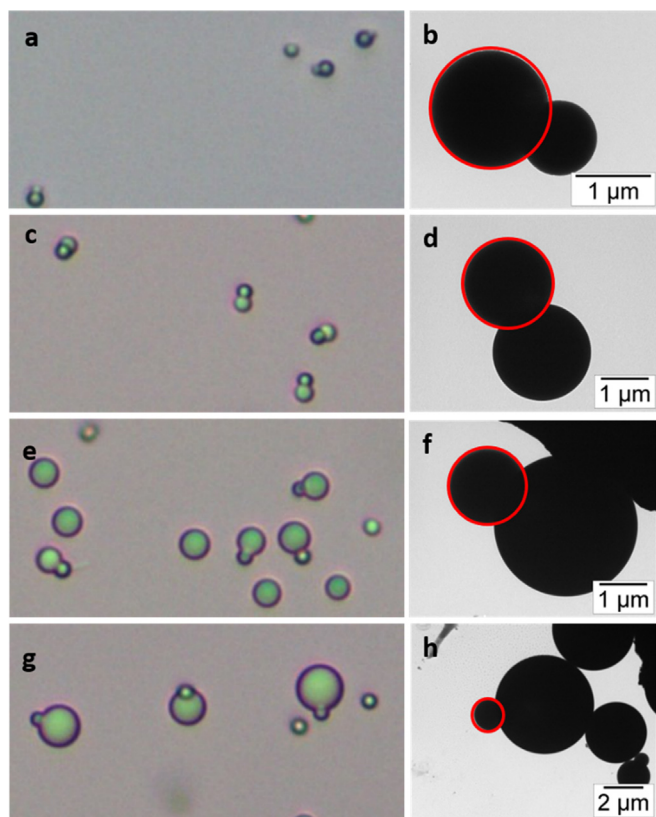


**Fig. 2.** Optical microscope images and transmission electron microscope (TEM) graphs of single-patch particles, showing that the size ratio of the two patches can be controlled by adding hydrolyzed 3-(trimethoxysilyl)propyl methacrylate (h-TPM) to the system. Examples of single-patch particles with the radius of the TPM lobe divided by the radius of the polystyrene seed ( $R_{\text{TPM}}/R_{\text{core-shell}}$ ) equal to (a, b) 0.38, (c, d) 1.1, (e, f) 1.8 and (g, h) 3.2. The brominated seeded patches are highlighted by the red circles.

relative size ratio of the two lobes. This was achieved by feeding various amounts of h-TPM to the system to grow the newly formed lobes into the desired size. Gradual TPM addition is preferred as it allows for better control over the geometry of the PS-p(TPM) hybrid particles and reduces the formation of secondary nucleation. As confirmed by optical and transmission electron microscopy (TEM) (Fig. 2), the relative size ratio, here defined as the radius of the TPM lobe divided by the radius of the polystyrene seed ( $R_{\text{TPM}}/R_{\text{core-shell}}$ ) was tunable over a wide range (0.38; 1.1; 1.8 and 3.2, respectively). Furthermore, TEM analysis revealed that the particles feature two well-defined spherical patches after polymerization.

**Synthesis of double-patch particle with variable geometry.** In addition to TPM, 3-(trimethoxysilyl)propyl acrylate (TMSPA) was employed as silane alkoxide monomer to generate anisotropic patchy particles. Interestingly, by substituting TPM for TMSPA, double-patch particles carrying two brominated seeded patches and a central p(TMSPA) lobe could be readily prepared. Approximately 40% of all colloids in a crude reaction mixture was a double-patch particle (Figure S3). Kraft *et al.* [5] showed that delaying the polymerization of liquid protrusions immobilized on colloidal particles led to coalescence of these liquid domains, leading to the formation of colloidal molecules. Similarly, the brominated seeds were fused by merging of the liquid TMSPA-oligomer droplets to form higher order patchy particles [5]. We found that the nucleation of hydrolyzed TMSPA (h-TMSPA) into protrusions is approximately 8 times slower than that observed for h-TPM. Compared to the relatively rapid nucleation reaction

of h-TPM, the slower nucleation and hence longer delay period before polymerization of the TMSPA droplet allowed particles to coalesce and form dimers bonded by a liquid TMSPA bridge (Fig. 3a). After fusion, the central TMSPA lobes gradually grow into a discrete central domain (Fig. 3b). Notably, the brominated seed particles were always in close proximity in the final cluster (Fig. 3). We attribute this geometric uniformity to strong capillary attractions generated between the seed particles when attached to the TPM-water interface. The necessity for slower hydrolysis rates to promote merging of liquid protrusions was confirmed by delaying the polymerization for the TPM-based procedure we presented in the previous section. In this case delayed polymerization led to formation of polydisperse clusters with ill-defined shapes.

Similar to the single-patch particles, where the size ratio between the TPM and PS-derived lobes could be tuned extensively (Fig. 2), the heterogeneous nucleation method enables the synthesis of double-patch particles having central TMSPA domains with dimensions controllable over a broad range (Fig. 3c-l). After merging of the liquid TMSPA protrusion localized on two different seeds, the central lobe can be grown to the desired size by sequential feeding of h-TMSPA. Accompanied with the growth of the central lobe is a decrease in the angle  $\theta$  between the brominated patches (Fig. 3b, inset). Angles ranging from nearly  $180^\circ$  (Fig. 3c, f) to  $20^\circ$  (Fig. 3g, l) are accessible. This variation in patch arrangement is extremely hard to realize for higher order patchy particles synthesized *via* conventional seeded dispersion/emulsion polymerization techniques [26–29].

**Orthogonal functionalization of anisotropic particles.** The hybrid colloids resulting from the polymerization of TPM or TMSPA contain two chemically distinctly patches: a silanol covered p(TPM)/p(TMSPA) lobe that can be easily modified with silane coupling agents, and a brominated lobe (PS-Br) containing alkyl bromides that can act as initiators for atom transfer radical polymerizations (ATRP). The difference in chemical nature between these two patches ensures that further modification can be performed independently and site-specifically. To confirm that the brominated moieties on the surface of the PS-Br core shell seeds remain localized on the patch and retain their functionality as ATRP initiators, these patches were labeled with 2-hydroxyethyl acrylate (HEA) and a fluorescent comonomer (methacryloxyethyl thiocarbonyl rhodamine B, (MTR)) (Fig. 4a). In agreement with our expectation, fluorescence microscopy revealed that only the region corresponding to the polystyrene patch was labeled after polymer grafting (Fig. 4c, f).

For the TPM/TMSPA-derived lobes, a variety of silane coupling agents can be utilized for selective modification. As an example, we used a fluorescent coupling agent to label the TPM/TMSPA lobe (Fig. 4a). Fluorescence microscopy shows that the larger p(TPM) lobe is clearly brighter than the PS-Br patch. This result suggests that the covalent silica modification is site-specific and localized on the anticipated patch (Fig. 4d, g). The weak fluorescence signal on the polystyrene patch is attributed to physical adsorption of the hydrophobic dye molecules (Fig. S4).

In addition to the fluorescent microscopy analysis, bright field optical microscopy and SEM analysis confirmed the site-specificity of the surface modification by revealing an increase in size and roughness of the brominated lobes after polymer grafting (Fig. 5). To facilitate the observation of the modified patches, polymer brushes with large thicknesses were targeted (Fig. 5b, e). The p(TPM) lobes were not affected by the ATRP reaction and remained smooth. The roughness of the polymer grafted patch in SEM (Fig. 5c, f) is caused by a collapse of the polymer brushes during sample preparation and imaging under vacuum. Naturally, ATRP grafting is not limited to HEA only. A wide variety of monomers can be polymerized using this technique, providing means to precisely tailor the chemistry of the polystyrene patch [30,31]. Nota-

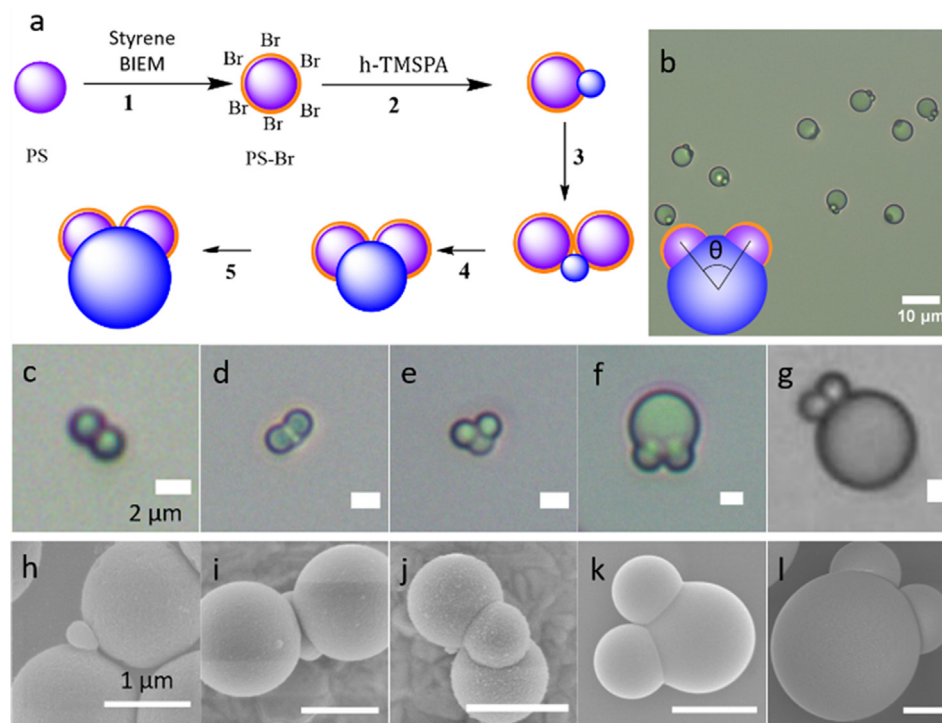


**Fig. 3.** (a) Schematic representation of the synthetic procedure toward double-patch particles with tunable geometries and patch arrangements. The brominated core-shell seeds prepared *via* seeded polymerization (Step 1) were dispersed in an aqueous solution containing hydrolyzed 3-(trimethoxysilyl) propyl acrylate (h-TMSPA) (Step 2). Spherical seeds partially engulfed by TMSPA oil droplets (in blue) coalesce with each other, forming dimers linked *via* liquid TMSPA domains (Step 3). The TMSPA oil droplet grows into the desired size by feeding fresh h-TMSPA before solidification *via* a free radical polymerization to obtain solid double-patch particles (Step 4, 5). (b) Representative optical microscope image of the polymerized double-patch particles after density gradient purification. The inset is a schematic representation of a double-patch particle carry two brominated polystyrene lobes. The relative orientation between the lobes is captured by the angle  $\theta$ . (c–g) Optical microscope images and (h–l) corresponding scanning electron microscope (SEM) images of double-patch particle with different angles. Scale bars of panels c–g = 2  $\mu\text{m}$ , and for panels h–l = 1  $\mu\text{m}$ .

ble examples of monomers used in combination with colloidal ATRP initiators are *N*-isopropylacrylamide [23], methyl methacrylate [24], glyceryl methacrylate [32] and [2-(methacryloyloxy)ethyl]trimethylammonium chloride [33].

To further probe the versatility of the functional groups on the particle surface, the terminal bromine atoms were substituted for azides by conducting a nucleophilic substitution reaction with sodium azide ( $\text{NaN}_3$ ). Introduction of the azide was confirmed by the presence of a diagnostic  $-\text{N}=\text{N}=\text{N}$  IR band at  $2150\text{ cm}^{-1}$  (Fig. 5h, pink spectrum). Substitution with azide groups enables further modifications using versatile Click Chemistry protocols [13,34]. Moreover, to show the reactivity of the p(TPM) patch, hexamethyldisilazane (HMDS) was used to modify the p(TPM) lobes. After modification three easily detectable characteristic bands of  $\text{Si}(\text{CH}_3)_3$  were observed in the IR spectrum (Fig. 5h, blue circle), providing proof that silane functionalization procedures can be applied to modify the TPM-derived patches.

**Reshaping colloids.** The seed-mediated heterogeneous nucleation procedures outlined here yields particles that contain highly crosslinked p(TPM) or p(TMSPA) patches and linear-core-shell brominated polystyrene domains. By exploiting the distinct difference in bulk (physical) properties of the lobes, the colloids can be reshaped into different morphologies [9]. For example, instead of polymerizing the TPM domains directly after the nucleation stage, the addition of small quantities of non-polymerizable toluene solvates the polystyrene patches. This results in a high mobility of the polymer chains and hence deformation of the particles into more spherical patchy colloids. The spherical shapes are favored as they ensure a minimization of the surface area and associated interfacial energy between the colloidal surface and dispersing medium. Distinct patches remain due to the immiscibility of the solvated seeds

and the TPM oil droplets (Fig. 6a, b). Based on this concept, Oh et al. [12] recently obtained particles with well-controlled Janus balance. The equilibrium shape of the multiphase particle depends on the amount of toluene added, which sets the contact angles between the three phases: water, TPM and toluene-swollen seeds [9]. Both single-patch (TPM-based) and double-patch (TMSPA-based) particles could be reshaped using this procedure.

The scope of reshaping the patchy particles with solvents can be extended by taking advantage of the core-shell structure of PS-Br. Chemical treatment with a mixture of ethanol and toluene induces selective dissolution of the polystyrene core, while leaving the brominated shell intact. The insolubility of brominated shell is in agreement with observations of Tanaka *et al.*, [35] who reported that even in the absence of chemical cross-linkers, P(S-BIEM) showed high resistance to organic solvents. After removal of the linear polystyrene core, the outer shell buckles and forms a dimpled structure. As shown in Fig. 6c, d, this procedure can be applied for both TPM and TMSPA based particles. The dimpled patchy particles could for example be used in depletion-guided assembly procedures to form higher order colloidal structures [36–38].

Another interesting class of colloids that can be assembled into well-designed structures *via* depletion forces are those consisting of both rough and smooth domains [39]. Because smooth surfaces have larger overlap volumes than rough surfaces, at appropriate depletant concentrations only the smooth lobes become attractive, generating directional interactions between the partially rough particles [39,40]. Although particles with site-specific surface roughness show great potential in self-assembly, [40,41] their synthesis remains difficult. Here, we demonstrate that we can readily modify the surface roughness of the seeds by varying the experimental conditions, such as the pH of the reaction medium and



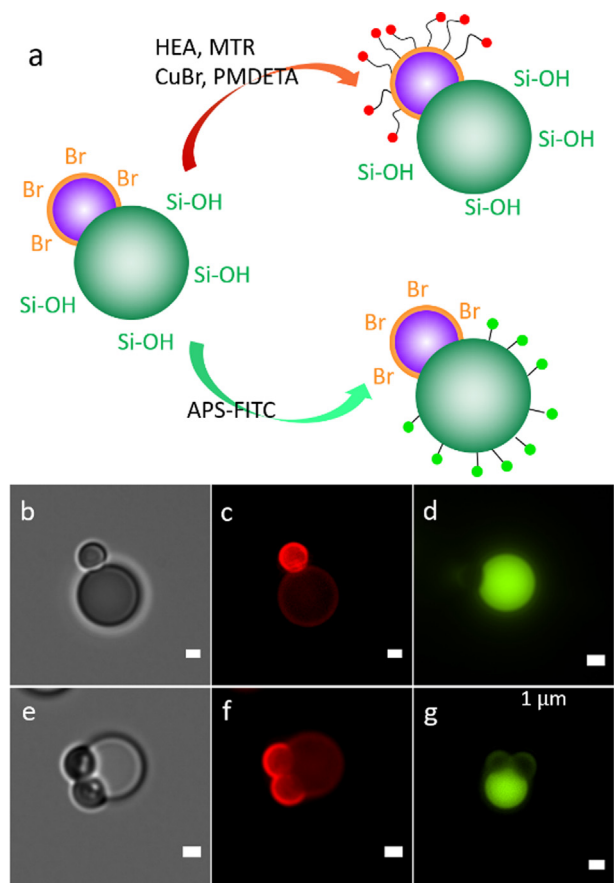


**Fig. 4.** (a) Schematic representation of orthogonal labelling of anisotropic single-patch and double-patch particles using atom transfer radical polymerization (ATRP) and silane chemistry with fluorescent monomers and silane coupling agents, respectively. (b, e) Brightfield optical microscope image of single-patch and double-patch particles. (c, f) Fluorescence microscopy images of particles labelled with methacryloxyethyl thiocarbonyl rhodamine B (MTR) by using ATRP. The red patches correspond to the functionalized PS-Br-derived patches. (d, g) Fluorescence microscopy images of functionalized p(TPM) or p(TMSPA) patches (in green) via silane chemistry using APS-FITC as dye. Scale bars = 1  $\mu\text{m}$ .

the initial amount of h-TPM/h-TMSPA [9]. At higher pH, the nucleation of h-TPM/h-TMSPA proceeds faster and the anisotropic particles tend to grow into raspberry-like particles rather than snowman-shaped colloids (Figure S2). Taking advantage of this feature, we controlled the morphology of the resulting snowman particles by inducing a second heterogeneous nucleation of h-TPM/h-TMSPA. After the formation of single- or double-patch particles, the second heterogeneous nucleation was performed at higher pH before solidifying the TPM or TMSPA lobes by polymerization. This strategy yields anisotropic particles featuring smooth TPM/TMSPA lobes and rough PS-Br-TPM/TMSPA patches decorated with multiple small p(TPM)/p(TMSPA) protrusions as illustrated in Fig. 6e, f.

#### 4. Conclusion

To conclude, this study outlines a novel and general route to fabricate bifunctional colloids featuring tailored anisotropy and functionality *via* a combination of seeded dispersion polymerization and heterogeneous nucleation. By using functional seed particles, a series of patchy particles with varying numbers of patches were prepared. The size and arrangements of the patches can be accurately adjusted by the total amount of monomer fed to the reaction system. Notably, compared to conventional dispersion [42,43] and emulsion [44,45] polymerization procedures towards

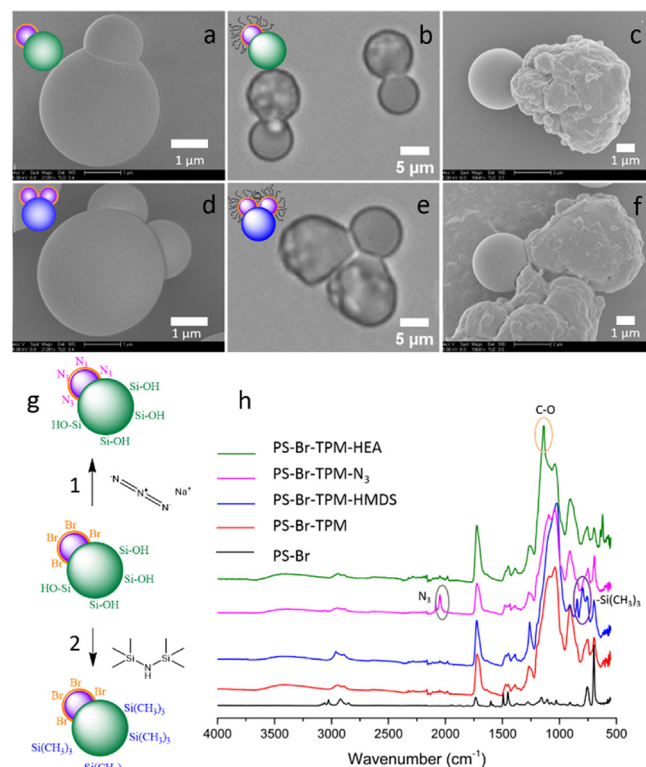


**Fig. 5.** Scanning electron microscopy (SEM) images of (a, d) anisotropic particles before modification. Optical microscope images (b, e) and SEM images (c, f) of particles modified with poly(2-hydroxyethyl acrylate) (p(HEA)) brushes grafted using ATRP. The smooth unmodified patch(es) corresponds to p(TPM) or p(TMSPA). (g1) Schematic representation of the substitution of surface bromine groups with azides and (g2) surface hydrophobization using hexamethyldisilazane (HMDS). (h) Infrared (IR) spectra of PS-Br seeds (black), PS-Br-TPM single-patch particles (red), PS-Br-TPM after surface modification with HMDS (blue), substitution with sodium azide ( $\text{NaN}_3$ , pink), and grafting with p(HEA) (green). The characteristic vibrational bands diagnostic for the modifications are highlighted with circles.

patchy particles, the method outlined here allows for controlling the morphology of the colloidal particles over a significantly broader window [7,46]. More importantly, we demonstrated that our strategy enables the synthesis of bifunctional colloidal molecules with chemically orthogonal patches. In particular, we synthesized particles carrying patches decorated with ATRP initiators and silanol functionalities. These functionalities allow for independent surface modification of all patches based on versatile controlled polymer grafting and silane chemistry, respectively. The orthogonal chemical character of our patches is a significant advancement in the synthesis of patchy particles, as previous systems are generally limited to having at least one chemically “inert patch” [42–45]. Additionally, we show that this morphological control and possibility for orthogonal surface modifications can be combined with the ability to reshape individual patches by site-selective polymerization and/or solvation. This greatly expands the library of accessible colloidal particles based on a single colloidal synthesis. Striking examples include the facile preparation of particles with dimpled or rough patches.

The morphological and chemical control provided by the reported synthesis will open new avenues for the bottom-up assembly of colloidal building blocks *via* directional interactions [14,36–37,39] or field-induced assembly [38,47,48]. For example, our procedure provides access to particles that not only mimic the shape but also the hydrogen bonding capabilities of water molecules. These colloidal analogues of water might shed light on the role of molecular geometry on crystalline and glassy phases of ice and undercooled water [49]. Furthermore, the applications of

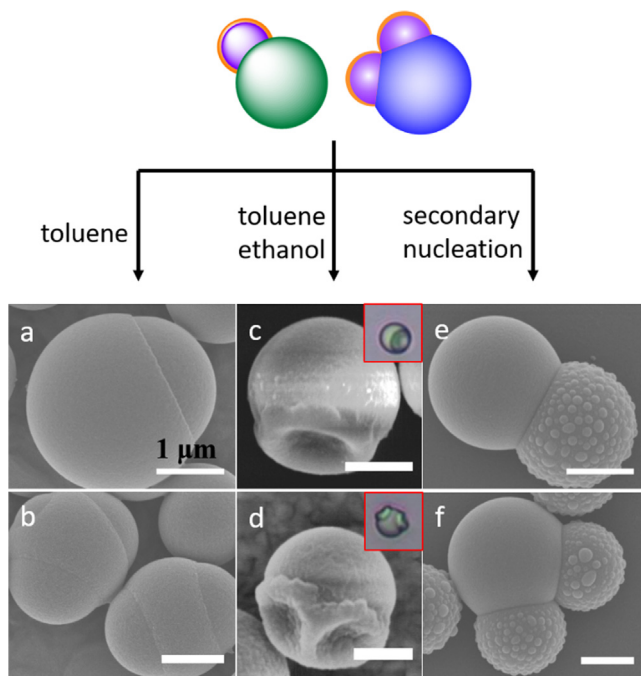


**Fig. 6.** Reshaping of particles via three different approaches. Single-patch particles with a p(TPM) lobe (a, c, e) and double-patch particles (b, d, f) with a TMSPA lobe. (a, b) Deformed single-patch and double-patch particles by using toluene to solvate the linear polystyrene seeds. (c, d) Hybrid dimpled particles featuring brominated dimples and spherical p(TPM)/p(TMSPA) patches obtained by using a mixture of toluene and ethanol to selectively dissolve the linear PS core of the PS-Br derived lobes. Insets: Optical microscope images of dimpled particles dispersed in water. (e, f) Particles with smooth p(TPM)/p(TMSPA) patches and rough polystyrene-derived lobes. The roughness is introduced by a second heterogeneous nucleation reaction of TPM/TMSPA performed at high pH. Scale bars = 1  $\mu\text{m}$ .

bifunctional colloids in tandem catalysis [50] or as multi-responsive self-propelling particles [51] by selectively grafting catalysts on different patches will be promising routes to explore in future work.

#### CRedit authorship contribution statement

**Fuqiang Chang:** Methodology, Investigation, Formal analysis, Writing - original draft, Writing - review & editing, Funding acquisition. **Samia Ouhajji:** Investigation, Writing - original draft. **Alice Townsend:** Methodology, Methodology. **Kanvaly Sanogo Lacina:** Formal analysis. **Bas G.P. Ravensteijn:** Formal analysis, Writing - review & editing. **Willem K. Kegel:** Supervision, Project administration.

#### Declaration of Competing Interest

The authors declared that there is no conflict of interest.

#### Acknowledgments

We acknowledge funding from the China Scholarship Council (CSC no. 201406230043). B. G. P. v. R acknowledges the Marie Curie Research Grants Scheme (Grant 838585 – STAR Polymers) for financial support.

#### Appendix A. Supplementary material

Supplementary data to this article can be found online at <https://doi.org/10.1016/j.jcis.2020.08.038>.

#### References

- [1] V.N. Manoharan, M.T. Elsesser, D.J. Pine, Dense packing and symmetry in small clusters of microspheres, *Science* 301 (80) (2003) 483–488.
- [2] N. Vogel, M. Retsch, C.-A. Fustin, A. del Campo, U. Jonas, Advances in colloidal assembly: the design of structure and hierarchy in two and three dimensions, *Chem. Rev.* 115 (2015) 6265–6311.
- [3] Kim, J.-W., Lee, D., Shum, H. C. & Weitz, D. a. Colloid Surfactants for Emulsion Stabilization. *Adv. Mater.* 20, 3239–3243 (2008).
- [4] J.-G. Park, J.D. Forster, E.R. Dufresne, High-yield synthesis of monodisperse dumbbell-shaped polymer nanoparticles, *J. Am. Chem. Soc.* 132 (2010) 5960–5961.
- [5] D.J. Kraft et al., Self-assembly of colloids with liquid protrusions, *J. Am. Chem. Soc.* 131 (2009) 1182–1186.
- [6] Kim, J., Larsen, R. J. & Weitz, D. a. Synthesis of Nonspherical Colloidal Particles with Anisotropic Properties. *J. Am. Chem. Soc.* 128, 14374–14377 (2006).
- [7] B.G.P. van Ravensteijn, W.K. Kegel, Tuning particle geometry of chemically anisotropic dumbbell-shaped colloids, *J. Colloid Interface Sci.* 490 (2017) 462–477.
- [8] H.R. Sheu, M.S. El-Aasser, J.W. Vanderhoff, Phase separation in polystyrene latex interpenetrating polymer networks, *J. Polym. Sci. Part A Polym. Chem.* 28 (1990) 629–651.
- [9] S. Sacanna et al., Shaping colloids for self-assembly, *Nat. Commun.* 4 (2013) 1688.
- [10] Z. Gong, T. Hueckel, G.-R. Yi, S. Sacanna, Patchy particles made by colloidal fusion, *Nature* 550 (2017) 234–238.
- [11] M. Youssef, T. Hueckel, G. Yi, S. Sacanna, Shape-shifting colloids via stimulated dewetting, *Nat. Commun.* 7 (2016) 12216.
- [12] J.S. Oh, S. Lee, S.C. Glotzer, G.-R. Yi, D.J. Pine, Colloidal fibers and rings by cooperative assembly, *Nat. Commun.* 10 (2019) 3936.
- [13] B.G.P. Van Ravensteijn, M. Kamp, A. Van Blaaderen, W.K. Kegel, General route toward chemically anisotropic colloids, *Chem. Mater.* 25 (2013) 4348–4353.
- [14] Y. Wang et al., Colloids with valence and specific directional bonding, *Nature* 491 (2012) 51–55.
- [15] Z. Luo, B. Liu, Shape-tunable colloids from structured liquid droplet templates, *Angew. Chemie – Int. Ed.* 57 (2018) 4940–4945.
- [16] Y. Sun, M. Chen, S. Zhou, J. Hu, L. Wu, Controllable synthesis and surface wettability of flower-shaped silver nanocube-organosilica hybrid colloidal nanoparticles, *ACS Nano* 9 (2015) 12513–12520.
- [17] A.H. Gröschel et al., Precise hierarchical self-assembly of multicompartment micelles, *Nat. Commun.* 3 (2012) 710.
- [18] F. Zhang, L. Cao, W. Yang, Preparation of monodisperse and anion-charged polystyrene microspheres stabilized with polymerizable sodium styrene sulfonate by dispersion polymerization, *Macromol. Chem. Phys.* 211 (2010) 744–751.
- [19] B.G.P. van Ravensteijn, W.K. Kegel, Versatile procedure for site-specific grafting of polymer brushes on patchy particles via atom transfer radical polymerization (ATRP), *Polym. Chem.* 7 (2016) 2858–2869.
- [20] A. Van Blaaderen, A. Vrij, Synthesis and characterization of colloidal dispersions of fluorescent, monodisperse silica spheres, *Langmuir* 8 (1992) 2921–2931.
- [21] D.B. Mahadik et al., Effect of concentration of trimethylchlorosilane (TMCS) and hexamethyldisilazane (HMDZ) silylating agents on surface free energy of silica aerogels, *J. Colloid Interface Sci.* 356 (2011) 298–302.
- [22] D.J. Kraft, J. Groenewold, W.K. Kegel, Colloidal molecules with well-controlled bond angles, *Soft Matter* 5 (2009) 3823.
- [23] F. Zhang, B.G.P. van Ravensteijn, K.S. Lacina, W.K. Kegel, Bifunctional janus spheres with chemically orthogonal patches, *ACS Macro Lett.* 8 (2019) 714–718.
- [24] B.G.P. van Ravensteijn, W.E. Hendriksen, R. Eelkema, J.H. van Esch, W.K. Kegel, Fuel-mediated transient clustering of colloidal building blocks, *J. Am. Chem. Soc.* 139 (2017) 9763–9766.
- [25] E.B. Mock, H. De Bruyn, B.S. Hawkett, R.G. Gilbert, C.F. Zukoski, Synthesis of anisotropic nanoparticles by seeded emulsion polymerization, *Langmuir* 22 (2006) 4037–4043.
- [26] D.J. Kraft et al., Self-assembly of colloids with liquid protrusions, *J. Am. Chem. Soc.* 131 (2009) 1182–1186.
- [27] Y. Sun, Interfaced heterogeneous nanodimers, *Natl. Sci. Rev.* 2 (2015) 329–348.
- [28] J.-W. Kim, R.J. Larsen, D.A. Weitz, Uniform nonspherical colloidal particles with tunable shapes, *Adv. Mater.* 19 (2007) 2005–2009.
- [29] J.-G. Park, J.D. Forster, E.R. Dufresne, Synthesis of colloidal particles with the symmetry of water molecules, *Langmuir* 25 (2009) 8903–8906.
- [30] K. Matyjaszewski, Atom transfer radical polymerization (ATRP): current status and future perspectives, *Macromolecules* 45 (2012) 4015–4039.
- [31] K. Matyjaszewski, Advanced materials by atom transfer radical polymerization, *Adv. Mater.* 30 (2018) 1706441.
- [32] S. Fujii, Y. Cai, J.V.M. Weaver, S.P. Armes, Syntheses of shell cross-linked micelles using acidic ABC triblock copolymers and their application as pH-responsive particulate emulsifiers, *J. Am. Chem. Soc.* 127 (2005) 7304–7305.
- [33] O. Glaied, M. Dubé, B. Chabot, C. Daneault, Synthesis of cationic polymer-grafted cellulose by aqueous ATRP, *J. Colloid Interface Sci.* 333 (2009) 145–151.
- [34] S. Ouhajji et al., Wet-chemical synthesis of chiral colloids, *ACS Nano* 12 (2018) 12089–12095.
- [35] T. Tanaka, M. Okayama, H. Minami, M. Okubo, Dual stimuli-responsive “mushroom-like” janus polymer particles as particulate surfactants †, *Langmuir* 26 (2010) 11732–11736.



- [36] Y. Wang et al., Three-dimensional lock and key colloids, *J. Am. Chem. Soc.* 136 (2014) 6866–6869.
- [37] S. Sacanna, W.T.M. Irvine, P.M. Chaikin, D.J. Pine, Lock and key colloids, *Nature* 464 (2010) 575–578.
- [38] M. Kamp et al., Electric-field-induced lock-and-key interactions between colloidal spheres and bowls, *Chem. Mater.* 28 (2016) 1040–1048.
- [39] D.J. Kraft et al., Surface roughness directed self-assembly of patchy particles into colloidal micelles, *Proc. Natl. Acad. Sci.* 109 (2012) 10787–10792.
- [40] M. Kamp et al., Selective depletion interactions in mixtures of rough and smooth silica spheres, *Langmuir* 32 (2016) 1233–1240.
- [41] J.R. Wolters et al., Self-assembly of “Mickey Mouse” shaped colloids into tube-like structures: experiments and simulations, *Soft Matter* 11 (2015) 1067–1077.
- [42] C. Anzivino et al., Equilibrium configurations and capillary interactions of Janus dumbbells and spherocylinders at fluid-fluid interfaces, *Soft Matter* 15 (2019) 2638–2647.
- [43] Z. Zhang et al., Controllable synthesis of anisotropic silica/polymer composite particles via seeded dispersion polymerization, *Mater. Chem. Phys.* 195 (2017) 105–113.
- [44] Y. Li et al., Morphology evolution of Janus dumbbell nanoparticles in seeded emulsion polymerization, *J. Colloid Interface Sci.* 543 (2019) 34–42.
- [45] Y. Liu et al., Preparation of Janus-type catalysts and their catalytic performance at emulsion interface, *J. Colloid Interface Sci.* 490 (2017) 357–364.
- [46] B. Peng, E. van der Wee, A. Imhof, A. van Blaaderen, Synthesis of monodisperse, highly cross-linked, fluorescent PMMA particles by dispersion polymerization, *Langmuir* 28 (2012) 6776–6785.
- [47] F. Ma, S. Wang, D.T. Wu, N. Wu, Electric-field-induced assembly and propulsion of chiral colloidal clusters, *Proc. Natl. Acad. Sci.* 112 (2015) 6307–6312.
- [48] F. Ma, S. Wang, L. Smith, N. Wu, Two-dimensional assembly of symmetric colloidal dimers under electric fields, *Adv. Funct. Mater.* 22 (2012) 4334–4343.
- [49] Salzmänn, C. G., Radaelli, P. G., Hallbrucker, A., Mayer, E. & Finney, J. L. The Preparation and Structures of Hydrogen Ordered Phases of Ice. *Science* (80-). 311, 1758–1761 (2006).
- [50] T. Yang et al., Dumbbell-shaped Bi-component mesoporous Janus solid nanoparticles for biphasic interface catalysis, *Angew. Chemie Int. Ed.* 56 (2017) 8459–8463.
- [51] S. Wang, N. Wu, Selecting the swimming mechanisms of colloidal particles: bubble propulsion versus self-diffusiophoresis, *Langmuir* 30 (2014) 3477–3486.